Talanta 87 (2011) 100–105

Contents lists available at SciVerse ScienceDirect

Talanta

journal homepage: www.elsevier.com/locate/talanta

Label-free immunoassay for chloramphenicol based on hollow gold nanospheres/chitosan composite

Ningdan Zhang, Fei Xiao, Jing Bai, Yanjun Lai, Jie Hou, Yuezhong Xian*, Litong Jin**

Department of Chemistry, East China Normal University, Shanghai 200062, PR China

ARTICLE INFO

Article history:
Received 18 May 2011
Received in revised form 22 July 2011
Accepted 28 July 2011
Available online 1 October 2011

Keywords:
Chloramphenicol
Immunosensor
Hollow gold nanospheres
Chitosan

ABSTRACT

A novel label-free electrochemical immunosensor for rapid determination of chloramphenicol (CAP) was fabricated by entrapping monoclonal antibody to chloramphenicol (anti-CAP) in hollow gold nanospheres (HGNs)/chitosan composite modified on a glassy carbon electrode. The hollow gold nanospheres (HGNs) were prepared by using Co nanoparticles as sacrificial templates and characterized by transmission electron microscopy (TEM). The changes of the electrode behavior after each fabrication step were investigated by electrochemical impedance spectroscopy (EIS) technique. Under optimal conditions, the proposed immunosensor has a sensitive response to CAP in a linear range of 0.1–1000 ng mL^{-1} with the detection limit of 0.06 ng mL^{-1}. Accurate detection of CAP in real meat samples was demonstrated by comparison with conventional HPLC method. The proposed method was proven to be a feasible quantitative method for CAP analysis with the properties of simple preparation, stability, high sensitivity and selectivity.

1. Introduction

Antibiotics are widely used in agriculture and aquaculture in order to deal with animal sickness and also as animal growth promoters. However, the use of antibiotics has created serious concerns regarding the drug residues present in animal-derived foods which would threaten public health [1].

Chloramphenicol (CAP) is one of the oldest antibiotics and was first isolated from *Streptomyces venezuelae* in 1947 [2,3]. CAP is a broad-spectrum antibiotic, active against both Gram-positive and Gram-negative bacteria. It exerts its action through inhibition of protein synthesis and is effective in the treatment of several infectious diseases. However, CAP is associated with serious toxic effects on human beings, which can result in bone marrow depression, particularly severe in the form of fatal aplastic anemia [4,5]. As a consequence, the use of CAP in food products has been banned in many countries. Nevertheless, CAP is still illegally used in animal husbandry because of its ready availability and low cost. Thus, a sensitive and accurate method for determination of CAP is needed.

The conventional method for CAP detection is high performance liquid chromatography (HPLC) coupled with different detectors, such as UV [6,7], MS [8,9]. Other analytical procedures, including isotope dilution [10], solid-phase extraction [11] and microflow chemiluminescence assay [12] have also been reported. Recently, a few electrochemical methods [13–15] based on the reduction of the nitro group in CAP have also been successfully applied in the detection of CAP. However, when CAP is mixed just in traces in food stuffs, developing more sensitive, selective and convenient methods for the determination of CAP is of great importance and interest.

Based on the high specific molecular recognition of the immunoreaction, immunosensors are very useful in widespread applications such as environmental monitoring [16], processing quality control [17], clinical diagnostics [18] and food safety test [19]. Compared with conventional bioanalytical methods used for CAP detection, such as enzyme-linked immunosorbent assay (ELISA) [20,21], the immunosensors based on surface plasmon resonance assay [19,22,23], piezoelectric quartz crystal [24,25] and electrochemistry [26,27] have got new development in recent decades. Among these methods, electrochemical immunosensors, combined the high specificity of traditional immunoassay methods with the low detection limits and low expenses of electrochemical measurement system, have gained growing attention. Several electrochemical immunosensors have been successfully developed for CAP detection with different types of electrodes, such as gold-magnetic nanoparticles modified electrode [26], cadmium sulfide nanoparticles and poly(amidoamine) dendrimers modified electrode [27]. A key issue with electrochemical immunosensor is the immobilization of immunological sensitivity compounds on the electrodes.

Gold nanoparticles (Au-NPs) have been extensively used in modification of various electrodes and fabrication of different kinds of biosensors with improved analytical performance by taking

* Corresponding author.
** Corresponding author. Tel.: +86 21 62232627; fax: +86 21 62232627.
E-mail address: ltjin@chem.ecnu.edu.cn (L. Jin).

0039-9140/$ – see front matter © 2011 Elsevier B.V. All rights reserved.
doi:10.1016/j.talanta.2011.07.108

advantage of the excellent biological compatibility, large surface area caused by a small granule diameter and the ability of promoting electron transfer [28,29]. However, common strategy for fabricating gold-based biosensors is mainly based on solid nanoparticles. Recently, nanomaterials with hollow interiors have attracted a great deal of attention due to their distinctive advantages of low density, high specific surface area, reduction of costs compared with their solid counterparts [30–32]. Hollow particles have been used for diverse applications, such as drug delivery [33], catalysis [32,34] and plasmonics [35]. In particular, hollow gold nanospheres (HGNs) have significant applications in optics and sensors due to their unique structural and optical properties, including high surface area, low density, and tunable SPR features [36]. In the field of DNA biosensor fabrication, Liu et al. [37] successfully developed a DNA biosensor with HGNs, and this sensor showed lower detection limit than that of other nanomaterials modified electrodes due to the high specific surface area of HGNs, which could enhance the DNA immobilization. However, to best of our knowledge, there is no report focused on the application of HGNs in CAP immunosensor. Therefore, it is necessary to explore this kind of special nanomaterial for the application in CAP immunosensor fabrication.

In this paper, a novel label-free electrochemical immunosensor based on HGNs/chitosan was constructed for the determination of CAP, which was realized by monitoring the change in the electrode response of $K_3[Fe(CN)_6]$ as the redox marker. The increase in CAP on the immunosensor inhibited $K_3[Fe(CN)_6]$ electron transfer and was detected as a reduction in electrochemical redox response. The HGNs were simply synthesized using a procedure that involved the template-engaged replacement reaction between Co nanoparticles and an aqueous $HAuCl_4$ solution, and characterized by transmission electron microscopy (TEM). Electrochemical impedance spectroscopy (EIS) and differential pulse voltammetry (DPV) were employed to investigate the electrochemical behavior of the electrodes, and the sensing range, sensitivity, and stability were determined. The proposed immunosensor was used for the determination of CAP in real meat samples.

2. Experimental

2.1. Chemicals and reagents

Monoclonal antibody to chloramphenicol (anti-CAP) was purchased from Hangzhou Clongene Biotech Co., Ltd. (Hangzhou, China). Chloramphenicol (CAP), bovine serum albumin (BSA) and Nafion were purchased from Sigma–Aldrich (USA). Tetrachloroaurate(III) tetrahydrate ($HAuCl_4{\cdot}4H_2O$), chitosan, glutaraldehyde and other reagents were purchased from Shanghai Chemical Factory (Shanghai, China). Phosphate-buffered saline (PBS buffer, 10 mM, pH 7.4) were prepared by varying the ratio of NaH_2PO_4 and Na_2HPO_4. All the reagents used were of analytical reagent grade and all solutions were prepared with pure water from Millipore (Milli-Q, 18.2 MΩcm).

2.2. Apparatus

DPV and EIS measurements were carried out on CHI 660A electrochemical workstation (CHI USA) with a three-electrode system, an anti-CAP/HGNs/chitosan modified electrode as working electrode, a saturated calomel electrode (SCE) as reference electrode and a platinum electrode as counter electrode. Transmission electron microscopy (TEM) was carried out on a JEOL JEM-2010 (JEOL Ltd. Japan). UV–visible spectroscopic data were obtained on a Cary 500 UV–vis–NIR spectrometer (Varian Comp, USA). HPLC analysis was carried out on LC10AT HPLC system (Shimadzu, Japan) with a UV detector.

2.3. Preparation of HGNs/chitosan composite

The synthesis of HGNs was carried out based on the reported method [38,39]. Briefly, 50 μL of 0.4 M $CoCl_2$ solution was added into 50 mL of deaerated aqueous solution containing 8 mM $NaBH_4$ and 0.8 mM citric acid to fabricate Co nanoparticles. High-purity nitrogen was bubbled through the solution during the whole procedure in order to avoid the oxidation of the Co nanoparticles in the existence of atmospheric oxygen. When the gas evolution ceased, 30 mL of as-synthesized Co nanoparticle colloidal solution was transferred to 18 mL of stirred 1 mM $HAuCl_4$ aqueous solutions to achieve the preparation of the HGNs. The obtained suspension solution was centrifuged at 10,000 rps and the precipitates were redispersed in 5 mL PBS (pH 7.4).

A 1% chitosan solution was prepared by dissolving 0.05 g of chitosan in 5 mL of 2% acetic acid solution (v/v). Then, 2 mL of colloidal HGNs was mixed with 1% chitosan solution. The mixture was continuously stirred for 2 h, and then it was placed at 4 °C overnight. Finally, the HGNs/chitosan composite was formed.

2.4. Preparation of CAP immunosensor

A glassy carbon (GC) electrode (Φ = 3 mm) was sequentially polished with 1.0, 0.3, and 0.05 μm Al_2O_3/water slurries, followed by successive sonication in HNO_3/H_2O (v/v, 1:1), NaOH (1 M), ethanol and water for 5 min and dried in air. A volume of 10 μL HGNs/chitosan composite solution, mixed with 2 μL glutaraldehyde (GA) solution (2.5%) was dropped onto the surface of the GCE, and allowed to dry at room temperature. Subsequently, 20 μL anti-CAP (40 μg mL^{-1}) was dropped onto the surface of the prepared electrode, then, the electrode was placed in a sealed tube and kept at 4 °C for about 2.5 h. After being rinsed with PBS, the formed anti-CAP/HGNs/chitosan modified electrode was incubated in 1.0% BSA solution for 0.5 h at 37 °C to eliminate nonspecific binding effect and block the remaining active groups, following by rinsing with PBS. The finished immunosensor was stored at 4 °C when not in use. The schematic illustration of the stepwise procedure for the immunosensor preparation was shown in Fig. 1.

2.5. Preparation of the meat samples

The beef, fish and pork samples were obtained from a market in China. Spiked meat samples were prepared by spiking appropriate amounts of CAP (10 μg g^{-1} in sample A, 20 μg g^{-1} in sample B and 50 μg g^{-1} in sample C) into meat. The preparation was done as follows, based on the procedure of Lee et al. [40]. Briefly, 0.5 g meat sample, 2.0 g of C18 powder, 0.05 g of oxalic acid, and 0.05 g of EDTA were mixed and homogenized completely using a pestle. Thereafter, the homogenized meat samples were loaded into a syringe column; liquated to 8.0 mL using 0.01 M methanolic oxalic acid and then dried under nitrogen. Then, the solution was used after melting of the concentrate with PBS buffer for the detection of CAP.

2.6. Detection of CAP by DPV

After the immunoreaction was performed by immersing the immunosensor in PBS (10 mM, pH 7.4) containing various concentrations of CAP for 20 min at 37 °C, and then washed carefully with PBS, DPV was used for the detection of CAP. The DPV experiments were performed in an unstirred 10 mL of 0.01 M PBS (pH 7.4) solution containing 0.1 M KCl and 2.5 mM $K_3[Fe(CN)_6]$ with the potential between −0.2 and 0.6 V (vs. SCE) at a scan rate of 50 mV s^{-1}.

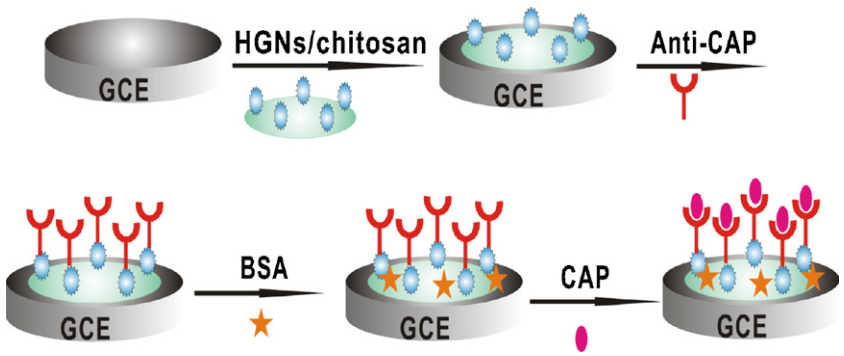

Fig. 1. Schematic illustration of the stepwise immunosensor fabrication process.

2.7. HPLC–UV analysis

CAP standard solutions or sample extracts were filtered through a 0.45 μm cellulose acetate membrane filter prior to HPLC detection. A HPLC system with a C18 column (3.5 μm, 150 mm × 4.6 mm) was equilibrated with mobile phase consisting of methanol/water (65/35, v/v) at a flow rate of 1.0 mL min^{-1}. The injection volume of standard or extract in each analysis was 20 μL. CAP was monitored at 280 nm by UV detector. The HPLC workstation software was used for the instrument control and data analysis. Peak areas were used for quantification.

3. Results and discussion

3.1. Characterization of HGNs and HGNs/chitosan composite

The HGNs were fabricated by using Co nanoparticles as sacrificial templates. The Co nanoparticles were synthesized with the reduction of Co^{2+} by $NaBH_4$. After the formation of Co nanoparticles, the solution was kept for several minutes to allow excessive $NaBH_4$ to react with water completely [32]. The standard reduction potentials of the $AuCl_4^-$/Au and Co^{2+}/Co redox couple are 0.994 and −0.277 V vs SHE. In the present study, the reduction potentials of these two redox couples can be obtained according to the Nernst equation. As the reduction potential of the $AuCl_4^-$/Au redox couple (0.935 V vs SHE) is much higher than that of the Co^{2+}/Co redox couple (−0.377 V vs SHE), the replacement reaction as presented in Eq. (1) will occur spontaneously as soon as $AuCl_4^-$ contacts with Co nanoparticles.

$$3Co + 2AuCl_4^- = 2Au + 3Co^{2+} + 8Cl^- \quad (1)$$

The structure and morphology of these HGNs were investigated by TEM. Fig. 2 exhibits a typical TEM image of as-synthesized HGNs, where there is a strong contrast difference in all of the spheres with a bright center surrounded by a much darker edge, which is in agreement with that in previous literature [39], confirming their hollow structure. The inset of Fig. 2 obviously shows hollow structure of gold spheres owned a rough outer surface. The average outer and inner diameters of these HGNs were measured to be approximately 23 and 10 nm, respectively. The prepared HGNs with rough surface should be very favorable for the application in biosensor fabrication due to its large surface area.

Due to the excellent film forming ability, chitosan with abundant amino-groups was used to functionalize HGNs for obtaining well-dispersed homogeneous suspension of HGNs/chitosan composite. To investigate the interaction of HGNs with chitosan, the UV–vis absorption spectra of the pure chitosan, pure HGNs, and HGNs/chitosan were studied, respectively (Fig. 3). As shown in Fig. 3, the spectroscopic response of chitosan solution did not show an absorption peak (curve a). While HGNs exhibited a distinct surface plasmon absorption band, with the maximum absorbance at about 600 nm (curve b). As for HGNs/chitosan, the characteristic absorption peak of HGNs was also observed (curve c). These results indicated that HGNs/chitosan was successfully formed.

3.2. Characterization of the electrode modification process

EIS is an effective method for probing the changes in the surface features of the modified electrodes in the assembly process

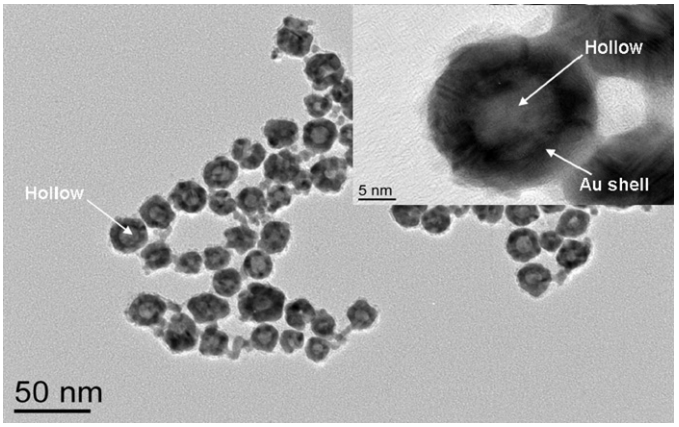

Fig. 2. Typical TEM image of hollow gold nanospheres.

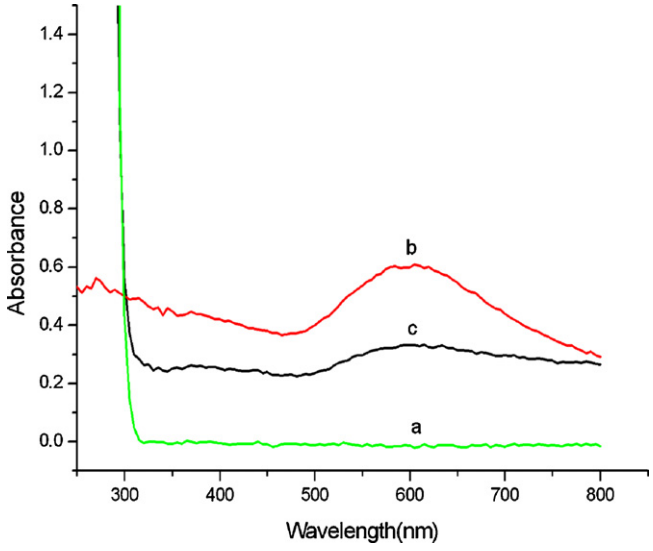

Fig. 3. UV–vis spectroscopy of (a) chitosan, (b) HGNs, (c) HGNs/chitosan.

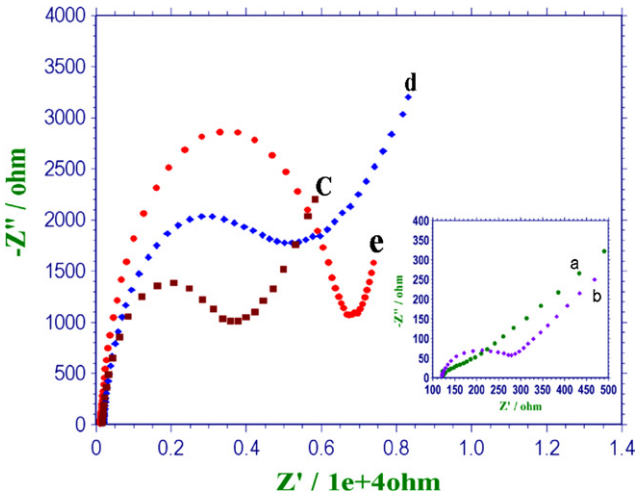

Fig. 4. EIS of (a) bare electrode, (b) HGNs/chitosan, (c) anti-CAP/HGNs/chitosan, (d) BSA/anti-CAP/HGNs/chitosan, (e) CAP/BSA/anti-CAP/HGNs/chitosan modified GC electrodes in PBS (10 mM, pH 7.4) containing 2.5 mM $[Fe(CN)_6]^{3-/4-}$ and 0.1 M KCl. The frequency range was from 10^{-1} to 10^5 Hz with alternative voltage of 5.0 mV.

[41,42]. The impedance spectra include a semicircle portion at higher frequencies corresponding to the electron transfer limited process, and a linear portion at lower frequencies representing the diffusion limited process. The semicircle diameter equals the electron-transfer resistance (R_{et}) [43]. Fig. 4 shows the Nyquist plots of EIS observed upon the stepwise modification processes in PBS (2.5 mM $[Fe(CN)_6]^{3-/4-}$ + 0.1 M KCl, pH 7.4). The bare GCE revealed a small semicircle domain (curve a), and the value of R_{et} was 69 Ω, implying a very low electron transfer resistance of the redox couple. After the electrode was modified with HGNs/chitosan composite, the value of R_{et} was 182 Ω, slightly bigger than that of bare GCE (curve b). The reason is that the existing chitosan acted as a barrier to the interfacial electron transfer, leading to an increase in R_{et}. Subsequently, CAP antibodies were combined on the HGNs/chitosan modified electrode and the R_{et} increased to 3639 Ω(curve c). A remarkable increase in R_{et} to 5342 Ω(curve d) was shown in successive step of BSA obturation. After the immobilization of CAP on the electrode, the value of R_{et} increased to 6755 Ω(curve e). The reason is that the antigen–antibody complex could act as the inert electron and mass transfer blocking layer, and it hinders the diffusion of ferricyanide toward the electrode surface significantly [42].

3.3. Optimization of experimental parameters

The environment temperature has significant effect on the activity of the antibody and antigen molecules. Thus, the influence of incubation temperature on the response signals for the antibody–antigen reaction was studied from 20 to 50 °C using the same CAP concentration (50 ng mL^{-1}). As shown in Fig. 5A, the response gradually decreased from 20 to 37 °C and then increased as the temperature further increased. It is believed that the anti-CAP on the electrode could be damaged at a high temperature. Thus, the incubation temperature of 37 °C was chosen for the subsequent assays.

Since it takes time for the anti-CAP immobilized on the electrode to react to the CAP molecules in the solution, the effect of the incubation time on the current response was carried out over the range of 0–30 min. With the increase of reaction time, the responses rapidly decreased and reached a plateau when the reaction time was longer than 20 min (Fig. 5B), indicating the CAP molecules in the solution were completely captured by the immobilized anti-CAP. As a result, 20 min was chosen to be incubation time in all of the subsequent experiments.

3.4. Determination of CAP

Under optimized experimental parameters, the DPV responses of the proposed immunosensor were obtained at different concentrations of CAP when the immunosensor was dipped into the PBS buffers containing $K_3[Fe(CN)_6]$ (Fig. 6A). Experimental results showed that the amperometric response of substrate was related to the amount of CAP adsorbed onto the electrode surface. With the increasing concentration of CAP, the response current was decreased gradually. The reason is that the increased immunocomplex of anti-CAP and CAP acted as the inert electron and mass transfer kinetic barrier, and decreased the effective area of the electrode surface and hindered the diffusion of ferricyanide toward the electrode surface [42]. The calibration plot for CAP under optimal experimental conditions is illustrated in Fig. 6B. A linear relationship between the amperometric response and logarithm of CAP concentration was obtained from 0.1 to 1000 ng mL^{-1} (R^2 = 0.9771), which was much wider than previous method [27]. The detection limit of the immunosensor was estimated to be 0.06 ng mL^{-1} at 3σ (where σ is the standard deviation of the blank, n = 15), which was better than or comparable to values found in the literature previously [26,27]. The wide linear rang and low detection limit of the proposed immunosensor might be attributed to the high specific surface area of HGNs, which could increase the sensoring surface

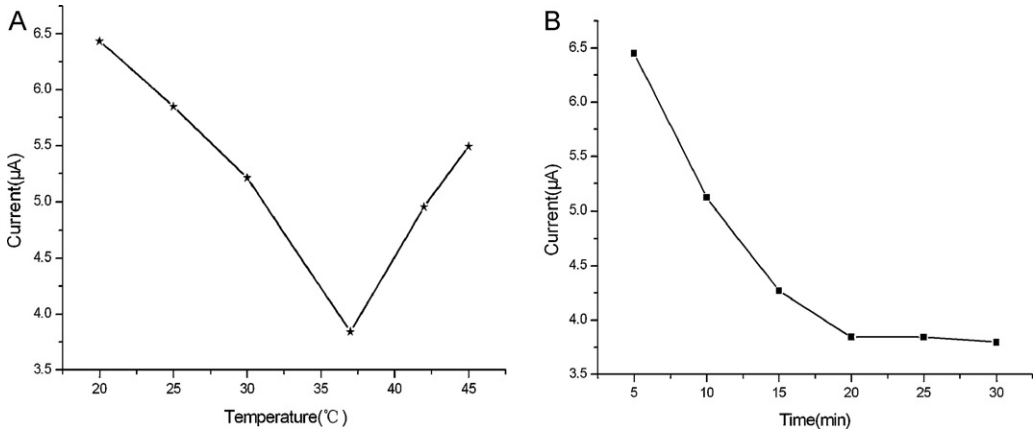

Fig. 5. Effect of incubation temperature (A) and immuno-reaction time (B) on DPV peak current of the immunosensor to 50 ng mL^{-1} CAP in PBS (10 mM, pH 7.4) solution containing 0.1 M KCl and 2.5 mM $K_3[Fe(CN)_6]$.

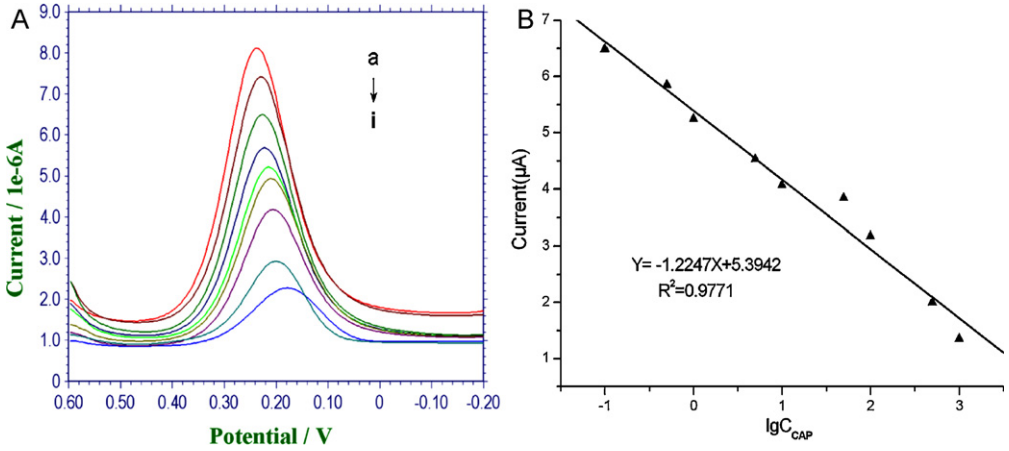

Fig. 6. (A) DPVs of the immunosensor with different concentrations of CAP on their surface in PBS (10 mM, pH 7.4) solution containing 0.1 M KCl and 2.5 mM $K_3[Fe(CN)_6]$: (a) 0.1, (b) 0.5, (c) 1, (d) 5, (e) 10, (f) 50, (g) 100, (h) 500, (i) 1000 ng mL^{-1}. (B) Calibration plots between the current response and the logarithmic value of CAP concentration.

areas, accordingly more anti-CAP could be absorbed on the electrode surface, and could enhance the access chance of the antigen and antibody.

3.5. Specificity, stability, reproducibility and regeneration of the immunosensor

The specificity of the immunosensor played an important role in analyzing real samples. To affirm the specificity of the CAP immunosensor, we chose streptomycin, ampicillin, tetracycline, neomycin as interferents to evaluate the specificity of the immunosensor. As can be seen in Fig. 7, when the immunosensors were respectively immersed in streptomycin, ampicillin, tetracycline, neomycin with same concentration (50 ng mL^{-1}), the current responses were not significantly affected (Fig. 7c–f), compared to the control experiment (Fig. 7a) in the absence of CAP and interferent. However, the current response decreases dramatically with 50 ng mL^{-1} CAP in the sample solution (Fig. 7b). Such selectivity reflected the highly specific binding affinity of the antigen–antibody immunoreactions, as well as the minimization of non-specific adsorption by the efficient blocking.

Additional experiments were carried out to test the reproducibility and stability. The reproducibility of the response currents of different immunosensors was made by the same procedure in 50 ng mL^{-1} CAP. The relative standard deviation was calculated to be 6.5% (n = 10). The CAP immunosensor was investigated one assay a day and stored in refrigerator at 4 °C to examine the long-term storage stability. The experimental results indicated that the current responses deviated only 10% (n = 20), indicating a good stability.

The regeneration of the immunosensor could be realized by rinsing with 0.1 M glycine–hydrochloric acid buffer solution (pH 2.8) to dissociate the antigen–antibody immunocomplex. After detecting 50 ng mL^{-1} CAP, the immunosensor was dipped into glycine–hydrochloric acid buffer solution for 5 min, removed to detect 50 ng mL^{-1} CAP, and repeated 5 times continuously. The experimental results indicated that the current responses deviated only 15% after five assay runs, showing accepted reusability.

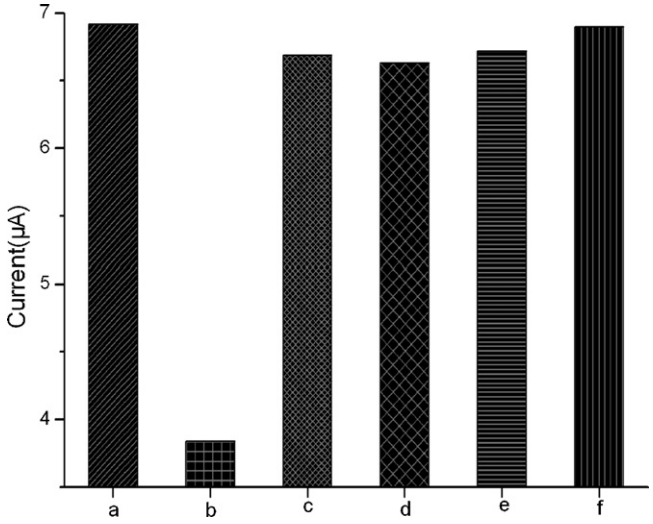

Fig. 7. Selectivity investigation of the immunosensor for (a) CAP (0 ng mL^{-1}) and interferent (0 ng mL^{-1}), (b) CAP (50 ng mL^{-1}), (c) streptomycin (50 ng mL^{-1}), (d) ampicillin (50 ng mL^{-1}), (e) tetracycline (50 ng mL^{-1}), and (f) neomycin (50 ng mL^{-1}).

Table 1
Recoveries of CAP from the spiked meat samples determined by immunosensor and HPLC–UV.

Sample	Spiked (μg g^{-1})	Immunosensor(n = 5)		HPLC–UV (n = 5)	
		Found (μg g^{-1})	Recovery (%)	Found (μg g^{-1})	Recovery (%)
Beef	10.00	9.35 ± 0.36	93.5	8.91 ± 0.23	89.1
	20.00	18.03 ± 0.52	90.2	17.69 ± 0.41	88.5
	50.00	43.76 ± 0.97	87.5	44.90 ± 1.34	89.8
Fish	10.00	9.04 ± 0.22	90.4	8.32 ± 0.37	83.2
	20.00	17.92 ± 0.45	89.6	18.47 ± 0.42	92.4
	50.00	42.57 ± 1.01	85.1	43.33 ± 1.29	86.7
Pork	10.00	9.26 ± 0.33	92.6	8.47 ± 0.29	84.7
	20.00	17.76 ± 0.54	88.8	17.69 ± 0.51	88.5
	50.00	45.52 ± 1.39	91.0	43.04 ± 0.98	86.1

3.6. CAP assay in real samples

The proposed anti-CAP/HGNs/chitosan/GCE immunosensor was applied to the determination of CAP in the beef, fish and pork samples using standard calibration curve. It was found that there was no CAP residue present in the meat samples. The recovery study was also performed by spiking meat samples with CAP at three different levels (10, 20 and 50 $\mu g\,g^{-1}$), according to the procedure described in Section 2.5. Five different samples of each concentration were independently processed. On the basis of the calibration curves, it was possible to calculate the recovery of the analyte, which ranged from 85% to 93%. The statistical results are summarized in Table 1. For comparison, the spiked samples were detected by the HPLC system. The results obtained with the HPLC are consistent with immunosensor results. Therefore, this method has good accuracy and great potential in the practice sample analysis.

4. Conclusions

The present work developed an electrochemical immunosensor for determination of CAP by immobilizing anti-CAP in HGNs/chitosan film. The average outer and inner diameters of these HGNs were measured to be approximately 23 and 10 nm by using TEM images. The prepared HGNs show a rough outer surface, which could increase the amount of antibody immobilized on electrode surface, providing higher sensitivity of the immunosensor. Under optimal conditions, the immunosensor could achieve a wide linear range from 0.1 to 1000 $ng\,mL^{-1}$ for CAP detection and low detection limit of 0.06 $ng\,mL^{-1}$. The immunosensor could be also suitable for the detection of CAP in meat samples with good precision, high sensitivity, acceptable stability and reproducibility. A satisfactory agreement of analytical results of the proposed method with those of HPLC shows good reliability of the method. Therefore, the developed method in this paper has the advantages of sensitivity, speed, and simplicity.

Acknowledgement

This work was supported by the National Natural Science Foundation of China (No. 20875031), Shanghai Rising-Star Program (No. 09QH1400800), and New Century Excellent Talents in University (No. NCET-09-0357).

References

[1] A.D. Corcia, M. Nazzari, J. Chromatogr. A 974 (2002) 53–89.
[2] A.A. Yunis, Annu. Rev. Pharmacol. Toxicol. 28 (1988) 83–100.
[3] D. Holt, D. Harvey, R. Hurley, Toxicol. Rev. 12 (1993) 83–95.
[4] M.F.W. Festing, P. Diamanti, J.A. Turton, Food Chem. Toxicol. 39 (2001) 375–383.
[5] M. Takino, S. Daishima, T. Nakahara, J. Chromatogr. A 1011 (2003) 67–75.
[6] C. Hummert, B. Luckas, H. Siebenlist, J. Chromatogr. B 668 (1995) 53–58.
[7] L.L. Wang, H. Yang, C.W. Zhang, Y.L. Mo, X.H. Lu, Anal. Chim. Acta 619 (2008) 54–58.
[8] R.S. Nicolich, E.W. Barroso, M.A.S. Marques, Anal. Chim. Acta 565 (2006) 97–102.
[9] J. Tuerk, M. Reinders, D. Dreyer, T.K. Kiffmeyer, K.G. Schmidt, H.M. Kuss, J. Chromatogr. B 831 (2006) 72–80.
[10] P.A. Guy, D. Royer, P. Mottier, E. Gremaud, A. Perisset, R.H. Stadler, J. Chromatogr. A 1054 (2004) 365–371.
[11] X.Z. Shi, A.B. Wu, S.L. Zheng, R.X. Li, D.B. Zhang, J. Chromatogr. B 850 (2007) 24–30.
[12] W. Thongchai, B. Liawruangath, S. Liawruangrath, G.M. Greenway, Talanta 82 (2010) 560–566.
[13] F. Xiao, F.Q. Zhao, J.W. Li, R. Yan, J.J. Yu, B.Z. Zeng, Anal. Chim. Acta 596 (2007) 79–85.
[14] J.C. Chen, J.L. Shih, C.H. Liu, M.Y. Kuo, J.M. Zen, Anal. Chem. 78 (2006) 3752–3757.
[15] L. Agüĭ, A. Guzmán, P. Yáñez-Sedeño, J.M. Pingarrón, Anal. Chim. Acta 461 (2002) 65–73.
[16] F. Long, M. He, H.C. Shi, A.N. Zhu, Biosens. Bioelectron. 23 (2008) 952–958.
[17] H.M. Nassef, M.C. Bermudo Redondo, P.J. Ciclitira, H.J. Ellis, A. Fragoso, C.K. O'Sullivan, Anal. Chem. 80 (2008) 9265–9271.
[18] S. Kumbhat, K. Sharma, R. Gehlot, A. Solanki, V. Joshi, J. Pharm. Biomed. Anal. 52 (2010) 255–259.
[19] F. Fernández, K. Hegnerová, M. Piliarik, F.S. Baeza, J. Homola, M.P. Marco, Biosens. Bioelectron. 26 (2010) 1231–1238.
[20] A.Y. Kolosova, J.V. Samsonova, A.M. Egorov, Food. Agric. Immunol. 12 (2000) 115–125.
[21] H.Y. Shen, H.L. Jiang, Anal. Chim. Acta 535 (2005) 33–41.
[22] J. Yuan, R. Oliver, M.I. Aguilar, Y.Q. Wu, Anal. Chem. 80 (2008) 8329–8333.
[23] S.R. Raz, M.G.E.G. Bremer, W. Haasnoot, W. Nrode, Anal. Chem. 81 (2009) 7743–7749.
[24] N. Adanyi, M. Varadi, N. Kim, I. Szendro, Curr. Appl. Phys. 6 (2006) 279–286.
[25] I.S. Park, D.K. Kim, N. Adanyi, M. Varadi, N. Kim, Biosens. Bioelectron. 19 (2004) 667–674.
[26] D.H. Xie, N. Gan, F. Wang, X. Yang, Chin. J. Sens. Actuators 22 (2009) 1371–1377.
[27] D.M. Kim, M.A. Rahman, M.H. Do, C. Ban, Y.B. Shim, Biosens. Bioelectron. 25 (2010) 1781–1788.
[28] N.D. Zhou, J. Wang, T. Chen, Z.G. Yu, G.X. Li, Anal. Chem. 78 (2006) 5227–5230.
[29] N. German, A. Ramanavicius, J. Voronovic, Y. Oztekin, A. Ramanaviciene, Microchim. Acta 172 (2011) 185–191.
[30] Y.G. Sun, Y.N. Xia, Anal. Chem. 74 (2002) 5297–5305.
[31] S.J. Guo, Y.X. Fang, S.J. Dong, E.K. Wang, J. Phys. Chem. C 111 (2007) 17104–17109.
[32] H.P. Liang, H.M. Zhang, J.S. Hu, Y.G. Guo, L.J. Wan, C.L. Bai, Angew. Chem. Int. Ed. 43 (2004) 1540–1543.
[33] E. Mathiowitz, J.S. Jacob, Y.S. Jong, G.P. Carino, D.E. Chickering, P. Chaturvedi, C.A. Santos, K. Vijayaraghavan, S. Montgomery, M. Bassett, C. Morrell, Nature 386 (1997) 410–414.
[34] S.W. Kim, M. Kim, W.Y. Lee, T. Hyeon, J. Am. Chem. Soc. 124 (2002) 7642–7643.
[35] S.J. Oldenburg, R.D. Averitt, S.L. Westcott, N.J. Halas, Chem. Phys. Lett. 288 (1998) 243–247.
[36] D.H. Wan, H.L. Chen, Y.S. Lin, S.Y. Chuang, J. Shieh, S.H. Chen, ACS Nano 3 (2009) 960–970.
[37] S.F. Liu, J. Liu, X.P. Han, Y.N. Cui, W. Wang, Biosens. Bioelectron. 25 (2010) 1640–1645.
[38] Y. Kobayashi, M. Horie, M. Konno, B. Rodríguez-González, L.M. Liz-Marzán, J. Phys. Chem. 107 (2003) 7420–7425.
[39] H.P. Liang, L.J. Wan, C.L. Bai, L. Jiang, J. Phys. Chem. B 109 (2005) 7795–7800.
[40] K.S. Lee, S.H. Park, S.Y. Won, Y.B. Shim, Electrophoresis 30 (2009) 3219–3227.
[41] X.H. Li, L. Dai, Y. Liu, X.J. Chen, W. Yan, L.P. Jiang, J.J. Zhu, Adv. Funct. Mater. 19 (2009) 3120–3128.
[42] A. Ramanavicius, A. Finkelsteinas, H. Cesiulis, A. Ramanaviciene, Bioelectrochemistry 79 (2010) 11–16.
[43] X.J. Chen, Y.Y. Wang, J.J. Zhou, Y. Wei, X.H. Li, J.J. Zhu, Anal. Chem. 80 (2008) 2133–2140.